

## Studies of Relativistic Uranium Nuclei with Dielectric Track Detectors

**Abstract.** *The cross section for the breakup of relativistic uranium projectiles (energy ~ 35 billion electron volts) into two large fragments in the track detector CR-39 was measured and found to be about half of the geometric cross section. The range of the uranium projectiles was also measured and found to agree with that predicted by the Bethe theory when modified to account for the capture of orbital electrons by the projectiles.*

To obtain graphic evidence for the acceleration of uranium nuclei to relativistic energies at the Bevalac (1) and to perform initial experiments with this previously unavailable radiation source, we exposed several stacks of polymeric track-etch detectors (2) to the uranium beam. We summarize here the results of two experiments performed with the track detector CR-39, whose properties have been described (2).

Figure 1 shows tracks of uranium projectiles in a CR-39 detector that was chemically etched in such a way as to discriminate in favor of highly ionizing particles. One can see examples of fragmentation of uranium into two and three highly charged fragments. Quantitative study of the etch rates, ranges, and angular distributions of the fragment tracks confirms that those are examples of binary and ternary fission of uranium induced by collisions with nuclei in the CR-39. From a total of 33 interactions in which two fragments were emitted, we determined the binary fission cross sec-

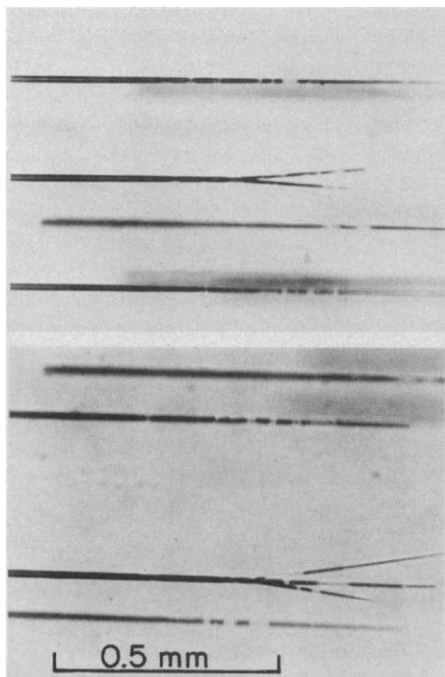


Fig. 1. Photomicrographs of etched tracks of  $^{238}\text{U}$  ions in CR-39. Examples of binary and ternary fissions are shown.

tion per CR-39 nucleus (composition  $\text{C}_{12}\text{H}_{18}\text{O}_7$ ) as  $1.37 \pm 0.40$  barns for uranium energies between 0 and 64 MeV/amu and  $1.41 \pm 0.31$  barns for energies from 66 to 121 MeV/amu. The fission cross section seems to be insensitive to energy and to be roughly half of the geometric cross section, which is calculated (3) to be 2.94 barns for  $^{238}\text{U}$  in CR-39. The one case of ternary fission occurred at an energy of 32 MeV/amu. The etch rate data indicate that the lightest of the three fragments had atomic number  $Z \approx 26$  and thus that the mass division was into three nearly equal fragments. Our results are consistent with those of Katcoff and Hudis (4), who studied the fission of stationary uranium nuclei by  $^{14}\text{N}$  ions and protons at an energy of 2.1 GeV/amu. In both cases they found fission cross sections to be roughly half of the geometric cross section. Our observation of one ternary and 33 binary fissions is consistent with their ternary-to-binary ratio of  $\sim 10^{-2}$  for  $^{14}\text{N} + \text{U}$ .

By measuring the penetration depth and lateral projection of the uranium tracks with a microscope, we found the average range in the CR-39 to be  $0.3771 \pm 0.0005$  g/cm<sup>2</sup>. By combining this thickness with that of an Al beam pipe window and a 56-cm flight path in air, we found the net range to be  $0.581 \pm 0.014$  g/cm<sup>2</sup>. The range straggling was found to be < 0.3 percent, which is consistent with that expected for very heavy projectiles. By using the algorithm of Barkas and Berger (5) to calculate the net range for  $^{238}\text{U}$  projectiles at 147.7 MeV/amu, we obtain the result of 0.580 g/cm<sup>2</sup>, which is remarkably close to the measured range. This was surprising in view of earlier work (6, 7) that confirmed the existence of higher order corrections to particle stopping power. For example, in Table 1 the discrepancies between the particle ranges and those predicted by the Barkas and Berger calculation are reproduced from (7) for relativistic neon, argon, and iron ions. These results indicate that the discrepancy increases with projectile charge, so that one might have expected a very large discrepancy for

uranium, contrary to our observations.

To emphasize the significance of these results, we review briefly the theory of the stopping power—that is, the rate of energy loss—of heavy ions in matter (8). We denote the stopping power of a projectile in an absorber by  $S \equiv dE/dx$ , where  $E$  is energy and  $x$  is distance. According to the first-order quantal result of Bethe (9),  $S = Z_1^2 f(\beta, Z_2)$ , where  $Z_1 e$  is the projectile charge,  $-e$  is the electron charge,  $\beta$  is the projectile velocity in units of the speed of light ( $c$ ), and  $Z_2$  is the atomic number of the absorber. Bethe's theory is expected to be valid only for  $\chi = Z_1/(137\beta) \ll 1$  and agrees very well with data on protons with energies from  $\sim 10$  to over 1000 MeV ( $0.05 > \chi > 0.01$ ). For larger  $\chi$ , deviations from the  $Z_1^2$  dependence predicted by Bethe have been observed. Since the Barkas and Berger calculations are based on Bethe's theory, the data from (7) are one example of such deviations. These data can be accounted for (7, 10) by using the exact Mott cross section (11) to evaluate ion-electron scattering probabilities rather than the first Born approximation employed by Bethe. This effectively yields a  $Z_1^3$  term in  $S$ . At lower velocities, Andersen *et al.* (6) measured  $Z_1^3$  and  $Z_1^4$  correction terms required for the evaluation of  $S$  for hydrogen, helium, and lithium ions at  $\sim 1$  MeV/amu. This  $Z_1^3$  correction is a low-velocity effect due to polarization of the target atoms by the projectile (12). The  $Z_1^4$  term is due to the Bloch correction (13). This was first calculated nonrelativistically and is due to the finite lateral extent of the wave packets of the absorber's electrons. It has been shown (10) that there is a relativistic component of the Bloch correction which almost cancels the nonrelativistic part for very fast heavy ions such as those in (7).

Table 1. Comparison of measured ranges from (7) with those calculated by the techniques in (5). The  $^{238}\text{U}$  result is from the present work.

Projectile type	Projectile velocity ( $c$ )	Absorber	Calculated range
			Measured range
$^{20}\text{Ne}$	0.794	Al	$1.008 \pm 0.002$
$^{20}\text{Ne}$	0.794	Cu	$1.006 \pm 0.002$
$^{40}\text{Ar}$	0.794	Al	$1.013 \pm 0.002$
$^{40}\text{Ar}$	0.794	Cu	$1.011 \pm 0.002$
$^{40}\text{Ar}$	0.794	Pb	$1.017 \pm 0.003$
$^{56}\text{Fe}$	0.794	Al	$1.020 \pm 0.003$
$^{56}\text{Fe}$	0.794	Cu	$1.019 \pm 0.003$
$^{56}\text{Fe}$	0.794	Pb	$1.025 \pm 0.004$
$^{238}\text{U}$	0.505	Al + air + CR-39	$0.998 \pm 0.024$

In addition to being sensitive to all of the corrections above, our uranium projectiles should be sensitive to the effects of electron capture and loss. Such was not the case for previous studies of higher order corrections. Studies of the charge state in air of uranium ions at 10 to 70 MeV yield a semiempirical expression (14) for charge state which, when extrapolated to 147.7 MeV/amu, indicates that about five electrons are captured by uranium projectiles. One can take the effect of charge state into account for calculations of  $S$  by replacing  $Z_1$  with  $Z_{\text{eff}}$ , the root-mean-square charge state of the ion. This is valid since the effective minimum impact parameter for scattering of electrons bound to the absorber material is typically larger than the orbits of electrons captured by the projectiles. To estimate the charge state of the uranium ions in this experiment, we used the expression for  $Z_{\text{rms}}$  given by Pierce and Blann (15), which is more suitable for solid absorbers than that in (14).

By including all the effects above except the relativistic Bloch correction (which cannot be calculated reliably for uranium), we calculate a net range for the uranium in this experiment to be 0.654 g/cm<sup>2</sup>, 13 percent larger than observed. By neglecting the higher order corrections, we obtain a result only 3 percent larger than observed. The latter result differs from the Barkas and Berger result due to the slightly different manner in which electron capture was taken into account. This indicates the sensitivity of the range calculation to this effect. Nevertheless, unless the energy of the <sup>238</sup>U is grossly incorrect (which seems unlikely since it was calculated from known magnetic fields, radio frequency, and flight paths), it seems that for 147.7 MeV/amu and below, all higher order corrections to  $S$  for uranium cancel.

Since the nonrelativistic Bloch correction far exceeds the polarization and Mott corrections at the relevant energies for the uranium beam, the relativistic Bloch correction must almost completely cancel the nonrelativistic Bloch correction, as was observed to be the case for the faster neon, argon, and iron beams (7, 10). Our calculations indicate that such magnitudes and sign of the relativistic Bloch correction are possible. It will be interesting to see if the cancellation of higher order terms continues to higher uranium energies as such beams become available.

It is apparent that theory does not provide reliable information on the stopping power of relativistic uranium ions and that an experimental approach is a

prerequisite to the interpretation of responses of detectors used to identify relativistic ultraheavy nuclei.

S. P. AHLEN

G. TARLÉ

P. B. PRICE

Department of Physics and Space  
Sciences Laboratory, University  
of California, Berkeley 94720

#### References and Notes

1. J. R. Alonzo *et al.*, *Science* **217**, 1135 (1982).
2. S. P. Ahlen, P. B. Price, G. Tarlé, *Phys. Today* **34** (No. 9), 32 (1981).
3. G. D. Westfall, L. W. Wilson, P. J. Lindstrom, J. H. Crawford, D. E. Greiner, H. H. Heckman, *Phys. Rev. C* **19**, 1309 (1979).
4. S. Katcoff and J. Hudis, *Phys. Rev. Lett.* **28**, 1066 (1972).
5. W. H. Barkas and M. J. Berger, *Natl. Acad.*

*Sci.-Natl. Res. Council. Publ.* 1133 (1964), p. 103.

6. H. H. Andersen, J. F. Bak, H. Knudsen, B. R. Nielsen, *Phys. Rev. A* **16**, 1929 (1977).
7. M. H. Salamon, S. P. Ahlen, G. Tarlé, K. C. Crebbin, *ibid.* **23**, 73 (1981).
8. S. P. Ahlen, *Rev. Mod. Phys.* **52**, 121 (1980).
9. H. Bethe, *Ann. Phys. (Leipzig)* **5**, 325 (1930); *Z. Phys.* **76**, 293 (1932).
10. S. P. Ahlen, *Phys. Rev. A*, in press.
11. N. F. Mott, *Proc. Cambridge Philos. Soc.* **27**, 553 (1931).
12. J. Lindhard, *Nucl. Instrum. Methods* **132**, 1 (1976).
13. F. Bloch, *Ann. Phys. (Leipzig)* **16**, 285 (1933).
14. H. D. Betz, G. Hartig, E. Leischner, C. Schmelzer, B. Stadler, J. Wehrauch, *Phys. Lett.* **22**, 643 (1966).
15. T. E. Pierce and M. Blann, *Phys. Rev.* **173**, 390 (1968).
16. We thank F. Lothrop and the Bevalac staff for their cooperation and T. Liss for assistance. This work was supported by the Department of Energy.

2 August 1982

## Nitrogen Fixation in the Marine Environment

**Abstract.** *Cyanobacteria of the genus Oscillatoria (Trichodesmium) account for annual inputs of nitrogen to the world's oceans of about  $4.8 \times 10^{12}$  grams while benthic environments contribute  $15 \times 10^{12}$  grams. The sum of these inputs is one-fifth of current estimates of nitrogen fixation in terrestrial environments and one-half of the present rate of industrial synthesis of ammonia. When the total of all nitrogen inputs to the sea is compared with estimated losses through denitrification, the marine nitrogen cycle approximates a steady state. Oceanic nitrogen fixation can supply less than 0.3 percent of the calculated demand of marine phytoplankton. The minor contribution by nitrogen fixation to the overall nitrogen economy of the sea is not consistent with the supposition that nitrogen is the primary limiting nutrient and suggests that factors other than nitrogen availability limit phytoplankton growth rates.*

Recent accountings of the global nitrogen cycle have uniformly relied on a limited number of studies in deriving their estimates of marine nitrogen fixation (1, 2). Relatively large errors and uncertainties are therefore inherent in these calculations. We now provide an estimate for marine nitrogen fixation based on intensive research into this process conducted over the last 15 years, along with existing information on the distribution and abundance of the predominating diazotrophic systems.

In the open ocean, high specific rates of nitrogen fixation have been associated with several species of free-living cyanobacteria in the genus *Oscillatoria* (formerly *Trichodesmium*) (3-7), epiphytes on the pelagic phaeophyte *Sargassum* (8), and bacteria and a cyanobacterium (*Richelia* sp.) endophytic in the diatom *Rhizosolenia* (5, 9). *Rhizosolenia*-associated nitrogen fixation has generally been detected only under bloom conditions (9), and available data do not suggest this to be a major source of combined nitrogen. For epiphytes on pelagic *Sargassum* sp., a minor overall input of  $0.018 \times 10^9$  g of nitrogen per year was computed from the seasonal abundances given for the North Atlantic and the Gulf

of Mexico (10) and an average rate of 18  $\mu\text{g}$  of nitrogen per gram (dry weight) per day derived from (8).

Studies on the abundance, productivity, and capacity for nitrogen fixation by pelagic marine *Oscillatoria* are widespread, spanning the major oceanic basins (3-7). Total nitrogen fixation computed from available data gave a total annual rate of 4.8 teragrams (Tg) ( $4.8 \times 10^{12}$  g) of nitrogen per year (Table 1). Highest rates occurred in the Indian Ocean during the northern monsoon, and overall the Indian Ocean had the highest annual rate of nitrogen fixation, followed by the Atlantic, then Pacific, oceans. As with the rhizobia of terrestrial ecosystems, a limited taxonomic group (*Oscillatoria* spp.) is responsible for a substantial fraction of the nitrogen fixation that occurs in the sea.

In benthic environments, studies have been carried out in deep sea (11), coastal (11-13), and estuarine (13, 14) sediments, as well as in sea grass (15), coral reef (16), salt marsh (17), and mangrove (18) communities (Table 2). Values have been scaled up with the use of current estimates of the extent of these areas (19-21). Overall, annual benthic nitrogen fixation is estimated to account for 15 Tg